

Influence of synthetic vegetation on suspended sediment capture in laboratory flume experiments

2018-19 Undergraduate Honors Thesis
Department of Geography
University of California, Berkeley



Justin Nghiem

Abstract some text for the abstract

1 Introduction

Sediment transport to coastal regions has wide consequences for key processes like land progradation, water quality, and ecological productivity. With the prospect of climate change and sea level rise looming, the significance of sediment load to coastal lands has grown considerably. Britsch and Dunbar [1993] found that an estimated 17.8 percent of land in a study area in the Louisiana Coastal Plain had been lost from the 1930s to 1990, with a maximum rate of land loss of about 42 mi² per year in 1974. This trend will be compounded in the near future as rates of relative sea level rise increase. The combination of erosion and submergence along the coast threatens not only its physical characteristics, but also its dense human environment and infrastructure. Coastal and deltaic zones are home to a large human population worldwide, on the order of hundreds of millions, and represent a rich social and economic network [Syvitski et al., 2009].

Improved understanding of sediment retention and transport through river deltas will be instrumental in answering these long-standing questions. In particular, past studies have explored the interactions between sediment particles and vegetation in ~~deltaic environments~~ and have found that the presence of vegetation in sediment-laden flows may enhance sediment retention by promoting deposition and direct adherence to vegetation stems [Fauria et al., 2015; Wu et al., 2011; Palmer et al., 2004].

Drawing on this work, laboratory flume experiments were performed in this study to infer the influence of vegetation on removal of suspended sediment in wetland flows. Two treatments in a recirculating flume were tested, one in which wooden dowels were installed to mimic wetland vegetation and one without dowels. A fixed sediment mass was added at the start of each experiment, and  sediment mass concentration was recorded over time. This study contributes to further understanding of sediment routing in wetlands by testing the influence of a large vegetation array at a higher water depth (greater than 30 cm). Previous studies have not addressed these  conditions, despite the observation that water depth in wetlands usually range up to 50 cm [Kadlec, 1990]. More concretely, the results of the experiments in this study, and future experimental and theoretical work, may inform wetland management to maximize sediment retention and mitigate land loss as part of the solution to the broader coastal conundrum.

2 Methods

2.1 Physical Setting

The removal of sediment in suspended load has been theorized as consisting of contributions of (1) direct interception (objects in the flow trap particles directly), (2) inertial impaction (particles with sufficiently large inertia deviate from flow lines and impact onto

objects that trap them), (3) gravitational deposition (particles settle on bed), and (4) diffusional deposition (particles impact and are trapped on objects from random motions) [Fauria et al., 2015]. In this study, direct interception and inertial impaction were the mechanisms of interest because of the focus on modeling vegetation effects.

2.2 Background Theory

2.2.1 Sediment Transport Model

The interaction of suspended particles transported in a flow and potential “collectors” (e.g. vegetation stems) in the flow may be modeled with probabilities of impaction and retention. The capture efficiency η is defined as the ratio of particle diameter and collector diameter [Palmer et al., 2004; Fauria et al., 2015]. The capture efficiency may be written as

$$\eta = \frac{b}{d_c} = P(\text{interaction with collector})$$

where b is the upstream width of flow transporting the particles that is undisturbed by the presence of the collector and d_c is the collector diameter (Figure 1).

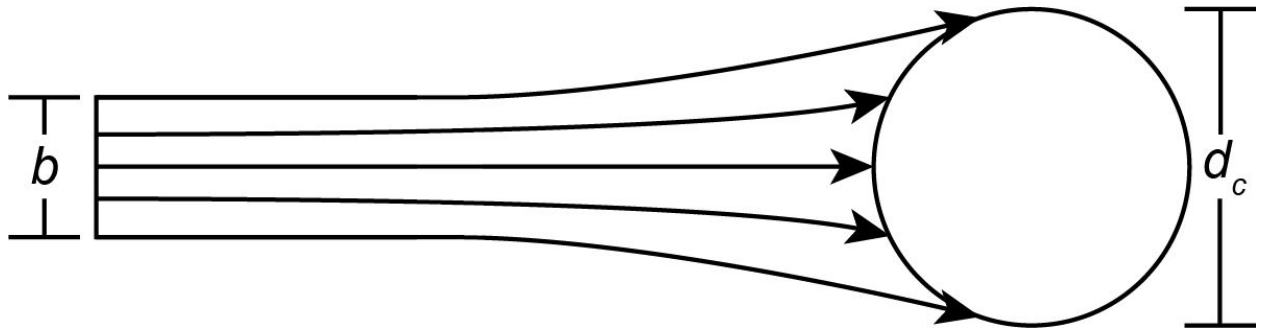


Figure 1. Illustration of particle capture efficiency. b is the upstream width of flow. d_c is the collector diameter. After Figure 1 in Palmer et al., 2004.

However, this formulation is solely a function of flow conditions and does not account for whether or not particles are retained on the collector. The effective capture efficiency η' rectifies this shortcoming by introducing an additional factor for the probability that a particle that impacts the collector is retained [Fauria et al., 2015],

$$\eta' = p_r \frac{b}{d_c} = P(\text{retention}|\text{interaction})P(\text{interaction with collector})$$

The effective particle efficiency, as defined above, quantifies the ability of a particular collector to remove suspended particles from the transported sediment load.

In order to quantify the changes in sediment concentration with time, a first-order relationship between these variables must be obtained. Fauria et al. [2015] describe the reduction in sediment concentration with time as an exponential decay, combining an advection-diffusion equation and the Rouse equation for suspended sediment profiles. This equation takes the form

$$\phi = \phi_0 e^{-kt}$$

where ϕ is the sediment concentration at some reference height above the bed, ϕ_0 is the initial sediment concentration at some reference height above the bed, k is the particle capture rate (s^{-1}), and t is time (s). The sediment concentrations may be volumetric or mass concentrations. For the purposes of this study, sediment concentrations were in units g/L or, equivalently, kg/m^3 . This equation implies that the particle capture rate may be estimated given measurements of sediment concentration with time at a reference height above the bed.

Additionally, Fauria et al. [2015] show that the particle capture rate k may be written as

$$k = k_s + k_c$$

where k_s is the particle capture rate attributable to gravitational settling of particles and k_c is the particle capture rate attributable to retention on vegetation features. This relation is valuable to disentangle the influence of vegetation collectors from gravitational deposition. In particular, k_c and effective capture efficiency are related, under further considerations of the Rouse equation and an advection-diffusion description of suspended sediment concentration, by the equation

$$\eta' = \frac{k_c}{ud_c l_c}$$

where u is the flow velocity (m/s) and l_c is the collector length per unit volume (m/m^3).

2.2.2 Stress Model

The law of the wall and Shields criterion were used to characterize the stress regimes in the flume leading to potential sediment transport. The equation for the law of the wall is

$$u(z) = \frac{1}{\kappa} u_* \log \frac{z}{z_0}$$

where u is the flow velocity as a function of elevation z from the bed (m/s), κ is the dimensionless von Kármán constant (taken to be 0.4), u_* is the shear velocity (the square root of the ratio of bed shear stress and fluid density; m/s), z is the elevation from the bed (m), \log denotes the natural logarithm, and z_0 is a characteristic length of bed roughness (m). The law of the wall assumes a turbulent flow regime, a requirement that is likely fulfilled from the Reynolds number (see section Flume Description). The statement of the law of the wall is useful because it quantifies the bed shear stress (through the shear velocity) once the flow velocity at a known height is measured.

Knowledge of the bed shear stress may then be applied in the Shields criterion for initial particle motion. The Shields criterion defines an empirical relationship between the particle Reynolds number, a function of the particle diameter, and the nondimensional critical shear stress at which a particle on the bed begins to move,

$$\tau_* = \frac{\tau_b}{(\rho_s - \rho_w)gD}$$

where τ_b is the bed shear stress, ρ_s is the sediment density, ρ_w is the fluid density (water in this case), g is gravitational acceleration, and D is particle diameter [García, 2008]. The relationship between particle Reynolds number and τ_* was approximated using an approximate mathematical relation [Brownlie, 1981]. The combination of the law of the wall and Shields criterion provided a more quantitative description of stress regimes and consequent sediment transport modes in the flume experiments.

2.3 Experimental Design

The goal of this study was to examine the influence of synthetic vegetation features in the removal of suspended particles in wetland environments. In order to respond to this question, two treatments were designed and performed. In all treatments, a fixed quantity of sediment was added to the flume and recirculated in flow conditions matching those of wetlands, and the change in sediment mass concentration with time was recorded over a period of 100 min. However, no dowels (proxies for vegetation) were present in the first treatment. In the second treatment, dowels were added to simulate the presence of vegetation. Detailed descriptions of each part of the experimental design follow in the remainder of this section.

2.3.1 Flume Description

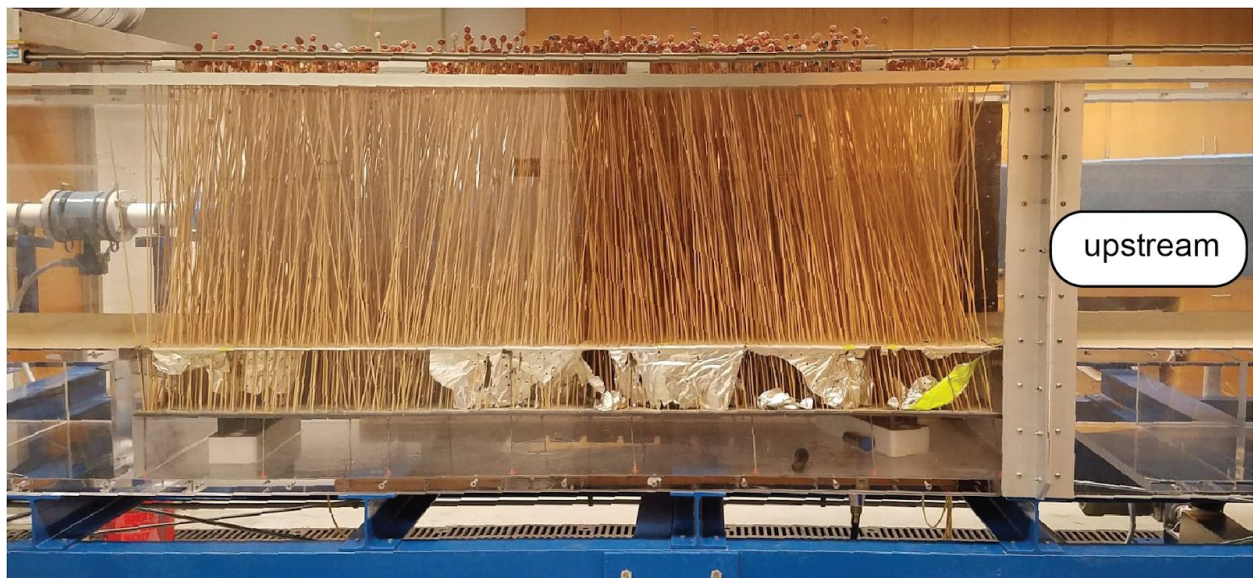


Figure 2. Side profile of recirculating flume used for the experiments. The open channel portion is pictured, with the dowels installed in the test section. The foil is visibly torn beneath the top of the PVC sheet because of dowel installation.

The laboratory experiments were performed in the ecogeomorphology recirculating flume in McCone Hall, Berkeley, CA. The flume consisted of an open channel (length 5.25 m, width 0.6 m, height up to 0.45 m) and a covered region to route water from the downstream end back to the upstream inlet. The flume had a single stand and close-coupled disc pump designed to pump fluids across low and high viscosities [Discflo]. The flume had an approximate maximum capacity of 3.1 m³ when filled to the maximum water depth of 45 cm. In addition, the open channel portion of the flume featured a removable false bed with the dimensions 0.6 m across the channel and 1.95 m along the channel (1.17 m²).

For all experiments in this study, the flume was operated with a water depth of 40 cm in the open channel segment, translating to an approximate flume water volume of 2.9 m³. The pump was set such that the average discharge of the flume was 0.0136 m³/s and the average flow velocity in the open channel portion was approximately 0.057 m/s. This flow velocity reflects moderate natural flow conditions in wetlands and is within the ranges of velocities examined in previous studies [Palmer et al., 2004; Fauriol et al., 2015]. The Reynolds number for a bare flume under these conditions, taking the characteristic length scale to be the hydraulic radius, is approximately 9749, indicating a transitional flow between turbulent and laminar regimes. Holding these flow conditions constant, the experimental treatments differed based on the presence of dowels acting as wetland vegetation.

2.3.2 Synthetic Vegetation Preparation

In order to model the presence of vegetation in the flow, wooden dowels were installed in the false bed portion in the flume (hereafter referred to as the “test section”). Individual dowels had an approximate diameter of 1/8 in. Dowels were placed upright in the test section through a perforated PVC sheet flush with the bed elevation upstream and downstream of the test section. The PVC sheet had regularly-spaced holes (diameter 0.1875 in) in a staggered pattern, with 0.313 in between the centers of any two adjacent holes. Before placing the PVC sheet in the flume, the sheet was wrapped in aluminum foil to limit unforeseen flows between the above and below bed regions through holes unoccupied by dowels. The dowels were additionally coated with a thin layer of silicone grease to mimic biofilms, then installed in the test section by puncturing through the foil into the holes in the PVC sheet.

The structure of the PVC sheet allowed for a maximum dowel density, defined as the number of dowels per area, of approximately 18,200 dowels/m² (e.g. every hole occupied). For the second treatment, the dowel density was approximately 1450 dowels/m² with the dowels placed in a uniform staggered pattern throughout the test section. The dowels were long enough such that they extended from the flume bed up past the water surface, thus imitating emergent vegetation. Small clay balls were added to the tops of all dowels to prevent the otherwise buoyant dowels from floating out of place. For the first treatment, no dowels were present in the test section. The bed surface of the test section in this treatment was the aluminum foil covering the PVC sheet.

Table 1. Summary of key experiment settings for all treatments. The only variable is the presence or absence of dowels in the test section. All numeric values are averages across the relevant spatial scale.

Treatment	Flow velocity (cm/s)	Dowel density (m ⁻²)	Sediment mass added (g)
1	5.7	0	200
2	5.7	1450	200

2.3.3 Sediment Preparation

The sediment used for the experiments in this study was 60/200 grade crushed walnut shell [Composition Materials]. The walnut shell had a specific gravity of approximately 1.3, and so was slightly denser than water [Composition Materials]. Sieve analysis shows that 94 to 96 percent of the walnut shell passes through a no. 60 sieve (250 µm sieve opening) and 3 to 5 percent passes through a no. 200 sieve (74 µm sieve opening) [Composition Materials].

The sediment was introduced into the upstream section of the open channel at the start of each experiment with a dispensing jug over approximately 3 minutes. A mass of 200 g walnut shell was well-mixed in about 4 gal of water in the jug before adding to the flume in each treatment. Previous tests with the flume showed that water recirculated back to the same point, under the given flow settings, in about 3 minutes. Thus, sediment addition using the dispensing jug ensured an approximately uniform initial sediment concentration throughout the flume.

The analytical distribution of crushed walnut shell diameters was estimated by assuming a normal distribution, fitting a normal CDF to the sieve analysis data (4 data points total), and inferring the parameters for a truncated normal distribution. Explicit measurements of the particle diameter distribution was not performed because of a lack of available tools to determine the distribution at a sufficient precision. The normal distribution was selected to model particle diameters because it describes a symmetric distribution with more weight concentrated about the mean, as is expected a priori in many particle size distributions. The manufacture process of the walnut shell was not expected to skew the particle diameter distribution to favor larger or smaller values, and so supported the assumptions despite the low number of data points. The estimation was performed by minimizing the residual sum of squares between the sieve analysis data points and the theoretical normal CDF. The result was an estimate of the mean and standard deviation of walnut shell particle diameters under a normal distribution. A truncated normal distribution, with a lower bound of 0 and an upper bound of twice the mean to preserve symmetry, was determined as the final model for the particle diameters. The truncated normal was selected to limit the support to physically meaningful sizes whereas the normal distribution has infinite support.

2.4 Instruments

In order to monitor and record necessary variables during the experiment, three instruments were used: (1) an acoustic Doppler velocimeter (ADV) to measure local flow velocities and (2) a pair of peristaltic pumps to measure sediment mass concentrations over time, and (3) a set of sediment traps to record particle settling in the test section.

2.4.1 Acoustic Doppler velocimeter

The ADV infers flow velocity at a point in three dimensions by using the Doppler effect to transform the change in pitch of a transmitted pulse as it is reflected by particles traveling in the flow into a flow velocity [Nortek]. As a result, the ADV relies on the assumption that particle velocity matches flow velocity. The ADV also features a temperature probe, which was used to record the average water temperature.

During the experiments, the ADV was mounted in the upstream portion of the open channel, about 1 m upstream from the edge of the test section in the center of the flow with the probe at 20 cm from the bed (Figure 3a). The ADV collected data throughout each experiment. Additional tests of the velocity field in the flume were conducted outside of the experimental treatments to better quantify flow velocities in more locations in the flume.

2.4.2 Peristaltic Pump Sampling

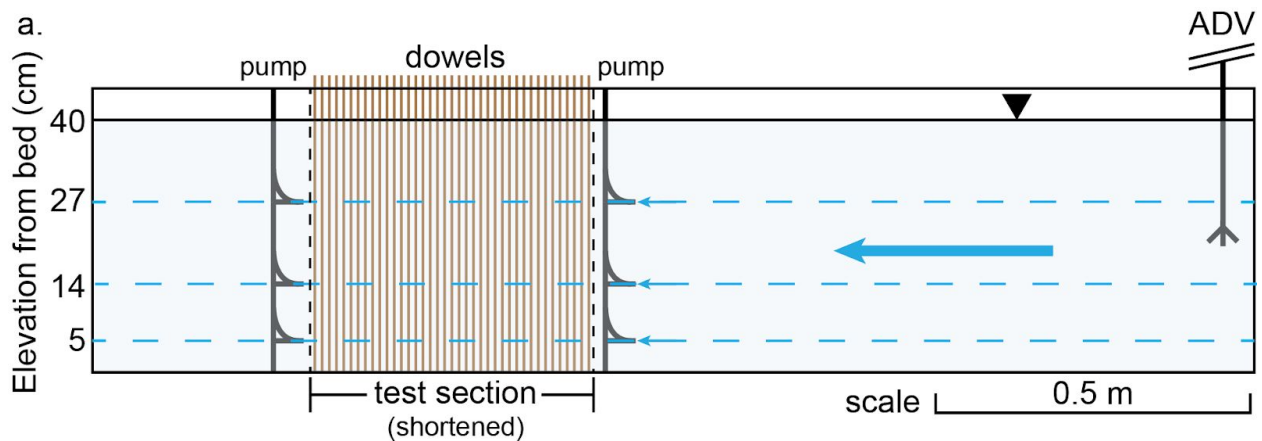
A pair of peristaltic pumps were installed to collect water samples from the flume along the open channel (Figure 3a). Each pump was connected to three hoses, which were routed to three sampling elevations in the flume (5 cm, 14 cm, and 27 cm from the bed) in the center of the flow. The opening of each hose in the flume was oriented pointing directly opposite and parallel to the direction of flow along the flume to maximize the representativeness of each water sample. This arrangement was placed at two locations in the flume, one immediately upstream of the test

section and the other immediately downstream of the test section. In sum, there were 6 distinct sampling regions in the flume (5 cm from the bed upstream of the test section, 14 cm upstream, 27 cm upstream, 5 cm downstream, 14 cm downstream, and 27 cm downstream).

Throughout each experiment, the peristaltic pumps continuously drained water from each of the sampling sites described at a flow rate of approximately 50 mL/min per hose. Water samples were collected for each sampling site at 5-min intervals for the duration of each experiment (100 min). All water samples were collected in clean plastic bottles and were typically filled to around 140 mL. The relatively low flow rate, combined with the addition of water when the sediment was introduced, implied that the net change in water in the flume over the course of an experiment was negligible.

2.4.3 Sediment Traps

Sediment traps were installed at nine well-spaced locations in the PVC sheet in the test section to collect samples of settling particles during the experiments (Figure 3b). Sediment traps were fabricated from cylindrical plastic syringe tubes with an approximate diameter of 2.5 cm. The syringe bottoms were replaced with perforated PVC, creating a depth of approximately 3.8 cm between the sediment trap opening and bottom. Before each experiment, each sediment trap was lined at the bottom with a glass microfiber filter paper and installed in the test section such that the sediment trap opening was effectively flush with the surface of the test section and exposed to the flow. During each experiment, particles settled into the sediment traps and collected on the filter paper. The perforated bottoms of the sediment traps were designed to better capture the amount of settled mass than a closed design, which would have required particles to displace water out of the sediment trap and would have underestimated the settled mass as a result. The relatively small diameter and modest number of sediment traps also limited any unforeseen mixing between the flow in the open channel and the reservoir below the surface of the test section that would have occurred with larger openings or more sample points.



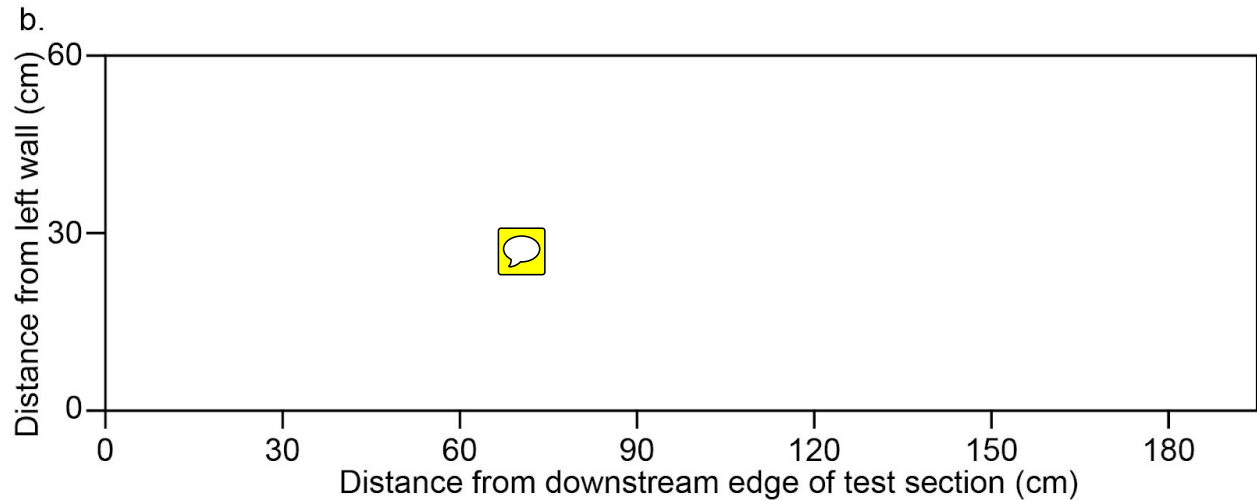


Figure 3. a. Schematic side profile of open channel portion for the dowel treatment. The uppermost 1.2 m in the upstream reach, lowermost 0.7 m in the downstream reach, and a 1.5-m stretch of the test section have been excluded from the view for clarity. All lengths are otherwise to scale. Peristaltic pumps and ADV were positioned in the center of the cross-flume width.
b. Overhead view of sediment trap positions in the test section. The test section was 1.95 m long and 0.6 m wide.

2.5 Filtering Protocol

After each experiment, the water samples from the peristaltic pumps were processed using a filtering protocol to determine the mass of sediment in each sample for its given volume. All water samples were filtered using a vacuum pump through glass microfiber filter paper that had been earlier heated in an oven at least overnight at 40°C to remove residual moisture. Each filter paper was weighed after heating and prior to a water sample being filtered through. The filter papers were then returned to the oven to remove excess moisture and re-weighed. The difference between the post-filtration mass and the pre-filtration mass of the filter paper was taken to be the collected sediment mass. The mass concentration of each sample was calculated to be this collected sediment mass divided by the measured volume of the sample. The result was a time series of mass concentration for each combination of sampling height and upstream/downstream location.

2.6 Statistical Methods

Although the bulk of the analysis methods so far has been without statistical methods to focus on physical means, such methods have been used in a few parts of the analysis in which it was most useful and illustrative to do so. First, as previously mentioned, the walnut shell particle diameter distribution was estimated parametrically by assuming a normal distribution on the sieve analysis data. Second, the parameters for the exponential decay model for suspended sediment were estimated using ordinary least squares (OLS). That is, ϕ_0 and k were estimated using an OLS procedure on the equation

$$\log \phi = \log \phi_0 - kt$$

in which $\log \phi$ is the natural logarithm of the initial concentration and $-k$ were the explicitly estimated parameters.

Finally, the Wilcoxon signed rank test was used to evaluate the statistical significance of the differences in mass concentration across upstream and downstream samples. Each pair was taken to be the samples with identical sampling height and time point, only differing in upstream/downstream location.

2.7 Separating the effects of settling and direct interception on collectors

For the treatment with dowels, the individual contributions of settling and interception on collectors were estimated using mathematical considerations of the background theory and measurements of settling from sediment trap data. The particle capture rate k may be partitioned into a rate related to particle settling (k_s) and a rate related to direct interception of particles on collectors (k_c), as seen from the background theory.

An equation is derived here to solve for k_c using a combination of known and estimated parameters in the experiments. The total mass settled throughout the flume during the experiment (m_s) is given by the integral

$$m_s = \int_0^T k_s m_0 e^{-kt} dt$$

where m_0 is the initial mass added to the flume and T is the length of time of the experiment. The initial mass times the exponential term models the overall decline in sediment mass over time due to deposition and capture on dowels, following the equation proposed by Fauria et al. [2015] with the exception that mass has been substituted in place of concentration. This expression for the sediment mass in the flow at a given time is multiplied by the capture rate constant due to settling (k_s) to give the instantaneous downward sediment mass flux. Then, the expression is time-integrated to yield the total mass settled over the course of the experiment.

The integral may be evaluated and the result rearranged to solve for the unknown k_s , which has the form

$$k_s = \frac{m_s k}{m_0 (1 - e^{-kT})}$$

in which all quantities on the right-hand side of the equation may be estimated from experiment data. The combined particle capture rate k was estimated, as described in a previous section, using mass concentration data from filtered water samples collected via the peristaltic pumps. The initial sediment added m_0 and the total time T of the experiment were recorded for each run. In all experiments in this study, the initial mass was approximately 200 g and the time for each experiment was approximately 6000 s.

Finally, the total mass settled in the flume during an experiment m_s was estimated using two data sources to account for different regimes of settling in the flume. First, spatial thin-plate spline interpolation of sediment trap data was used to quantify settling in the test section in which the dowels were expected to influence the pattern and intensity of settling compared to an empty test section. Second, the simple average settling recorded by the sediment traps in the run without dowels was scaled by area to estimate the amount of sediment settling in the open channel regions outside of the test section in the run with dowels. It was assumed that no settling

occurred outside of the open channel portion of the flume, a choice that was justified because flow velocities were elevated in those regions because of smaller cross-sectional area.

3 Results

3.1 Parametric Estimation of Particle Diameter Distribution

A normal CDF was fit, with the residual sum of squares as the loss function, to the sieve analysis data for the 60/200 crushed walnut shell that was used as sediment in the flume experiments (Figure 4). The fitted normal distribution had a mean of about 165.08 μm and a standard deviation of about 52.17 μm (Figure 4). The coefficient of determination (R^2) for the model was approximately 0.9999, indicating a very close fit to the sieve analysis data. The final model was a truncated normal distribution with the aforementioned mean and standard deviation with support in the interval 0 to 330 μm to avoid negative values and maintain symmetry.

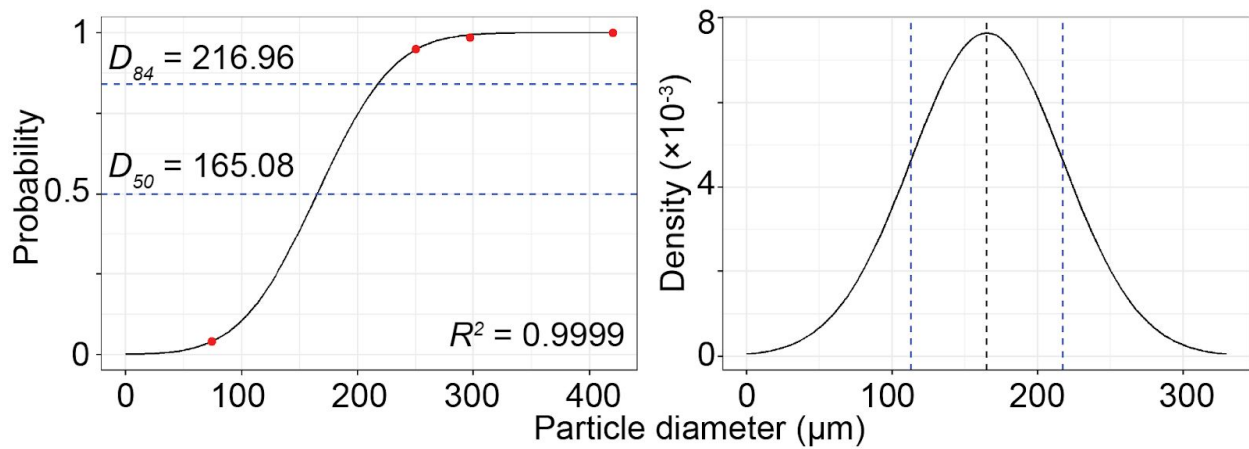


Figure 4. Left: estimated normal CDF. D_{50} (median) and D_{84} particle diameters are marked by the horizontal dashed lines.

Right: estimated normal PDF. The blue dashed lines mark one standard deviation above and below the mean. The black dashed line marks the mean.

3.2 Stress Conditions

The stress conditions were computed for two locations in the flume. The first location was 1 m upstream from the edge of the test section in the center of the flow, which was taken to be representative of regions of steady flow without the influence of dowels. The second location was well within the interior of the test section in the presence of dowels in the center of the flow, which was taken to be representative of regions in the test section in the experiment with dowels in which dowels interacted with the flow.


The shear  velocities at these two locations were estimated using the law of the wall and ADV readings of the local flow velocity at a given height. In the calculations, the characteristic bed roughness length z_0 was taken as 269.43 μm , which was two standard deviations above the mean from the derived particle diameter distribution. Additionally, the values for the density and kinematic viscosity of water were assumed for a water temperature of 20°C, which was supported by temperature readings from the ADV.

Table 2. Estimated shear-related parameters from Shields analysis. The listed diameters were the threshold maximum diameters of particles that would begin to move by fluid force at the given shear stress. The error bounds were the twice the sample standard deviation of measurements at a given location.

Region description	Shear velocity ($\times 10^{-3}$ m/s)	Bed shear stress ($\times 10^{-2}$ Pa)	Particle diameter (μm)
Upstream, no dowels	3.943 ± 0.254	$1.552 \pm 6.449 \times 10^{-3}$	16.18
Test, dowels	3.762 ± 1.637	1.413 ± 0.268	14.03

The similarity in estimated shear parameters indicated that the presence of dowels had a minimal effect on transport conditions (Table 2). In the upstream region without dowels, the estimated shear velocity was 3.943×10^{-3} m/s, translating to an approximate bed shear stress of 0.01552 Pa (Table 2). Under this stress, the critical particle diameter for initial motion was estimated as 16.18 μm . In the test section with dowels, the identical procedure led to estimates of 3.762×10^{-3} m/s for shear velocity, 0.01413 Pa for shear stress, and 14.03 μm for critical particle diameter. The error bounds, which were computed from twice the standard deviation of continuous flow velocity measurements at given locations, indicated that the shear velocities and bed shear stresses were within the range of being indistinguishable from each other by location, supporting the notion that dowels had a negligible influence on shear stress conditions at the resolution of the ADV.

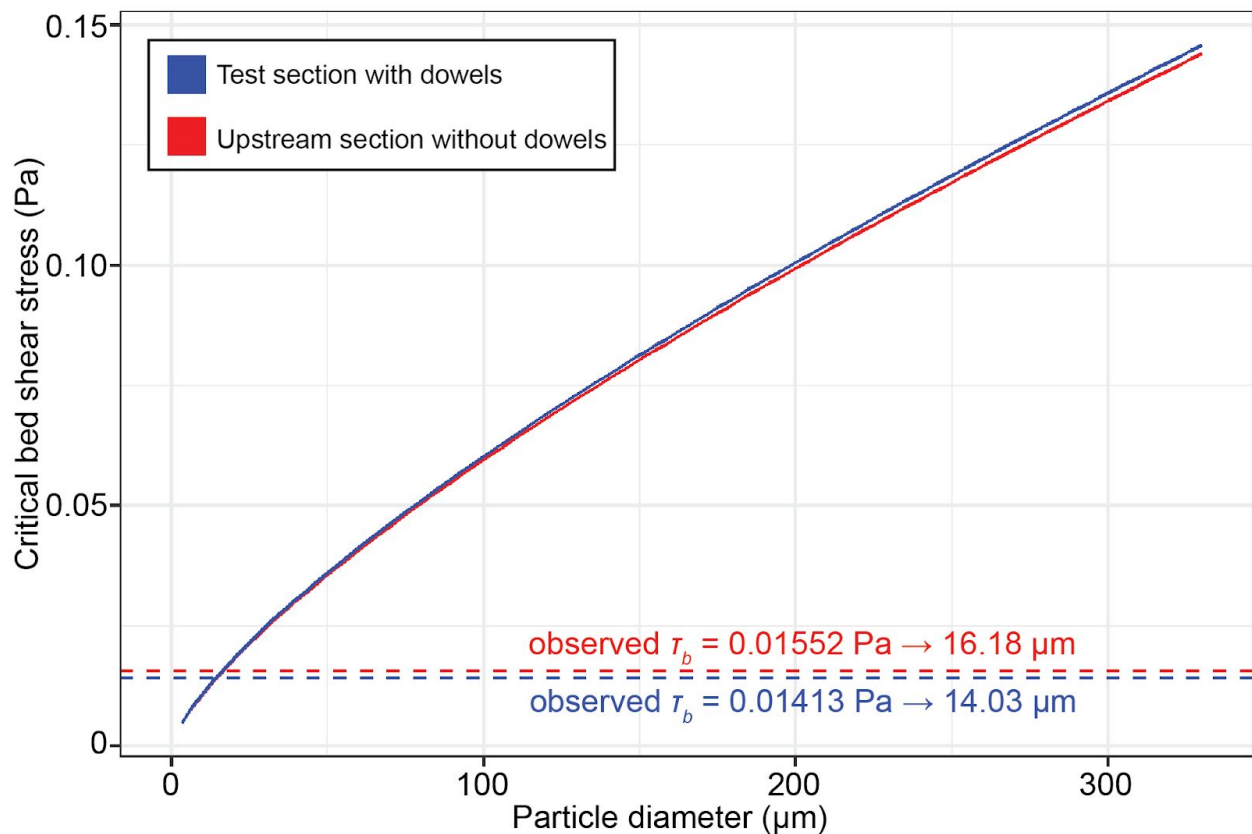


Figure 5. Critical shear stress for initial particle motion as a function of particle diameter for 0 to 330 μm . The dashed red lines mark the observed bed shear stress and the corresponding particle diameter for each of the two regions.

The Shields criterion was applied to infer a general transport description for the range of walnut shell particle sizes. Using the Shields criterion, the critical bed shear stress for initial particle motion as a function of particle diameter (0 to 330 μm) was enumerated (Figure 5).

In general, the relationship of particle diameter and critical stress was again similar across locations indicating that dowels had a marginal effect on the mode of sediment transport. The observed bed shear stress was only large enough to initiate motion from the bed of particles up to about 14 to 16 μm depending on the region in question. This range of particle diameters, using the parametric distribution estimate, exceeded approximately 0.2 percent of the size distribution. In other words, only 0.4 g out of a 200 g sample of the walnut shell were, on average, smaller than the critical particle diameter and the remainder were larger.

This information revealed that, for the vast majority of the particles, once they had settled on the bed, very little resuspension occurred because the particles were too large to be moved by the shear stresses in the flume regardless of the presence of dowels. In addition, these magnitudes of remobilization were conservative because shear velocity was measured in the center of flow where shear velocity tends to be maximized due to reduced wall drag. With this conclusion, the sediment transport setting of the experiments may be described as dominated by a declining suspended load over time with little evidence for appreciable bed load. The further analysis focused on the rate of change of this suspended load in the presence or absence of vegetation proxies in the form of dowels.

3.3 Treatment Comparison

Table 3. Estimated treatment parameters with uncertainty bounds equal to twice the corresponding standard error.

Treatment	Initial concentration (g/L)	Particle capture rate k ($\times 10^{-4} \text{ s}^{-1}$)
1 (no dowels)	49.80 ± 2.02	1.620 ± 0.0601
2 (dowels)	51.55 ± 2.03	2.229 ± 0.0924

The treatment with dowels had, compared to the treatment without dowels, a faster decline in mass concentration over the length of the experiments (Figure 6). Accordingly, the estimated particle capture rate k for the dowel treatment was $2.229 \times 10^{-4} \text{ s}^{-1}$ ($R^2 = 0.9603$; Table 3) which was greater than that for the no dowel treatment at $1.620 \times 10^{-4} \text{ s}^{-1}$ ($R^2 = 0.9506$; Table 3). These differences in the particle capture rate between runs were distinguishable as evidenced by the relatively tight uncertainty bounds, obtained from the model fit, which did not overlap (Table 3). In contrast, the initial concentrations were well within bounds of each other and thus indistinguishable, a result which was expected because an identical sediment mass was added at the start of each run. The high coefficients of determination for both treatments supported the validity of the theoretical exponential model for suspended sediment removal.

In support of the conclusion drawn from the quantification of particle capture rate, the dowel treatment had a visibly faster decline in mass concentration (Figure 6). From a more physically meaningful perspective, the time-averaged difference in concentration between the

treatments in the final 10 minutes of the experiments (5400 to 6000 s) was 5.31 g/L, found by integrating the exponential models.

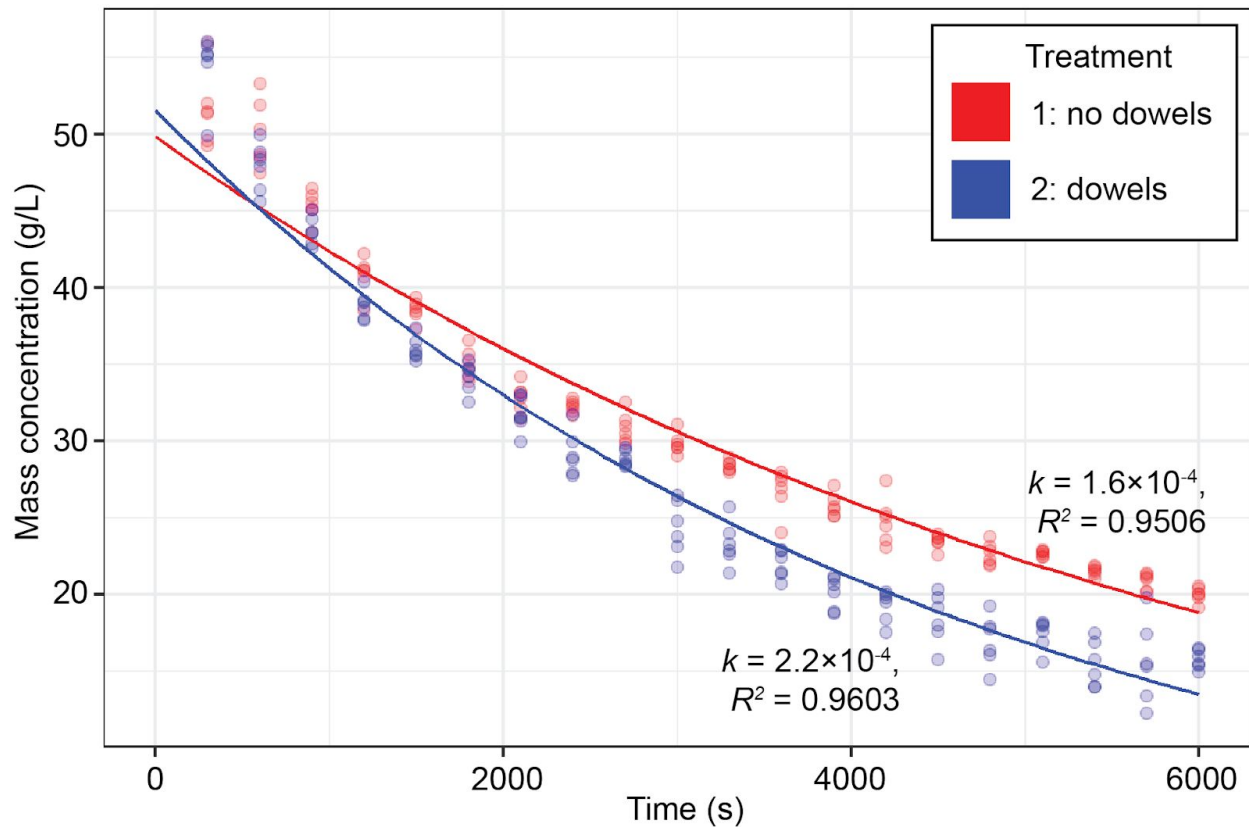


Figure 6. Time series of mass concentration for the treatments. The points do not distinguish between sampling height and longitudinal location.

The treatment results showed an appreciable difference in particle capture rates. However, an additional question for the dowel treatment was whether there was a difference in mass concentrations between the upstream and downstream sampling sites. Theoretically, the presence of the dowels in the test section would enhance particle removal so the upstream concentration should be consistently larger than the downstream concentration for the same time point. The mean of the paired differences of the upstream and downstream concentrations was 0.274 g/L, indicating that the upstream concentration was slightly larger on average.

In order to evaluate the significance of this difference, the Wilcoxon signed rank test was used. The null hypothesis was that the difference was equal to 0 (indistinguishable upstream and downstream concentrations). The alternative hypothesis was that the difference was greater than 0 (upstream concentration larger than downstream concentration). The test yielded a p -value of 0.336, meaning that there was little evidence in the data to support the claim that the upstream concentration was significantly larger than the downstream concentration.

Despite the result of the test, there was no decisive evidence that the difference between upstream and downstream concentrations was negligible. For example, the current dataset may not have been large enough to detect significant differences on the order of tenths of g/L. Another consideration was that the sampling interval and recirculation period were too coarse to

fully identify the difference. Specifically, the time to fill a water sample was approximately 2 to 3 minutes while the time for a parcel of water to make one circulation was approximately 3 minutes. The overlap between these time scales may have obscured potential larger differences in the upstream and downstream samples.

3.4 Particle capture rates and effective capture efficiency

Table 3. Estimated particle capture parameters with uncertainty bounds equal to twice the corresponding standard error. Intervals in brackets denote asymmetric uncertainty bounds.

Treatment	$k (\times 10^{-4} \text{ s}^{-1})$	$k_s (\times 10^{-4} \text{ s}^{-1})$	$k_c (\times 10^{-4} \text{ s}^{-1})$	$\eta' (\%)$
1 (no dowels)	1.620 ± 0.0601	1.620 ± 0.0601	0	0
2 (dowels)	2.229 ± 0.0924	0.4213 [0.4122, 0.4305]	1.808 [1.706, 1.909]	0.0689 [0.0650, 0.0728]

Following the procedures outlined in Methods, the sediment mass that settled during the run with dowels was estimated as 27.88 g (15.94 g in test section, 11.94 g in remainder of the flume open channel). From these values, the particle capture rate due to settling was estimated to be $4.213 \times 10^{-5} \text{ s}^{-1}$ for the dowel treatment (Table 3). The difference of the total particle capture rate k and this value yielded an estimate of the capture rate due to direct interception on collectors, which was $1.808 \times 10^{-4} \text{ s}^{-1}$. The calculated k_c was then used to compute the effective capture efficiency η' , yielding a value of 0.0689%.

For the treatment without dowels, the estimated overall particle capture rate k was equal to the capture rate due to settling because of the absence of collectors. Nominally, the effective capture efficiency was also 0 for the same reason of the absence of collectors.

The influence of the dowels was observed from comparisons of the capture rates. Within the dowel treatment, the capture rate due to dowels was an order of magnitude larger than the capture rate due to settling. Furthermore, the capture rate due to settling in the no dowel treatment was comparable to the capture rate due to dowels in the dowel treatment. It then also followed that the settling capture rate in the dowel treatment was an order of magnitude smaller than that of the no dowel treatment.

4 Discussion

4.1 Capture mechanisms and their interaction

Overall, the larger capture rate in the dowel treatment compared to the no dowel treatment indicated that the dowels, at the given density and preparation with silicone grease in this study, increased the ability of the flume system to retain sediment. Even more, the partition of the capture rate between settling and direct interception provided evidence for specific sediment capture mechanisms. In the dowel treatment, the estimated particle capture rates suggest that direct interception on dowels was the dominant sediment removal mechanism rather than gravitational deposition because of the order of magnitude difference in capture rates ($4.213 \times 10^{-5} \text{ s}^{-1}$ for settling against $1.808 \times 10^{-4} \text{ s}^{-1}$ for direct interception).

The results of the dowel treatment indicated that the introduction of dowels led to an interaction with settling such that the capture rate due to settling was reduced compared to that in the no dowel treatment. In other words, the dowels did not simply add to the total capture rate with a constant capture rate due to settling but rather influenced the settling itself. This

interaction was observed through the fact that the settling capture rate in the dowel treatment was one order-of-magnitude smaller in comparison to the corresponding result in the no dowel treatment. One interpretation is that the presence of dowels generated flow instabilities, introducing greater turbulence (e.g. in the form of turbulent eddies and wakes downstream of dowels). These turbulent elements then tended to loft suspended particles away from the bed, thus inhibiting gravitational settling of particles and decreasing the settling capture rate.

The results potentially support the idea that the presence of vegetation stems in the flow reduces shear velocities by introducing greater skin friction and drag, thereby decreasing flow velocity and shear stresses. The recorded shear velocity among the dowels (0.003762 m/s) was smaller than that in an upstream location free of dowel interference (0.003943 m/s). However, this difference was small and the computed error bounds were unable to distinguish the two measurements as appreciably different from each other. If any differences were present, then the ADV did not have the requisite resolution to identify them.

However, vegetation stems in flow have competing effects on particle capture. On one hand, they reduce cross-sectional area of the flow and increase flow velocity, leading to conditions in which more sediment may be transported. But they may also facilitate settling and deposition of particles by increasing drag against the flow and thereby reducing flow velocities. The presence of vegetation (and dowels) then is a tradeoff between turbulence and particle deposition. Indeed, Nepf [1999] modeled turbulence and drag in flows with varying arrays of emergent vegetation and found that the intensity of turbulence initially increases with greater vegetation density because of wake generation and then decreases as greater drag slows flow velocities. In this framework, the dowel treatment may be viewed as falling under conditions that promote turbulence and, as a result, reduce deposition. The validity of this proposition is potentially evidenced by the observed reduction in shear velocity within the dowels as compared to shear velocity free of dowels, but this was again subject to question of error.

4.2 Comparison to Published Literature

The calculated effective capture efficiency for the dowel treatment in this study (0.0689%) was comparable to values obtained by workers in past studies, although it was among the range of smaller values. Effective capture efficiencies in other studies have ranged from approximately 0.02 to 0.7% across many vegetation densities and flow velocities [Fauria et al., 2015; Purich, 2006].

A concrete comparison to previous findings may be made using Fauria et al.'s [2015] empirical equation for effective capture efficiency. The authors found that, for the stem density 7209 m⁻² and presence of biofilm in flume experiments using emergent vegetation,

$$\eta' = 2.06 Re_c^{-1.14} R^{0.65}$$

where Re_c is the collector Reynolds number and R is the ratio of particle diameter and collector diameter. For the conditions in the dowel treatment, the collector Reynolds number was approximately 180.6 and R was approximately 0.0520 (taking the mean particle diameter as a representative value). The corresponding predicted effective capture efficiency was about 0.0807%. The prediction matches well with the observed effective capture efficiency in this study, being on the same order of magnitude and slightly greater than the observed value, and validates the findings of this study compared to previously published studies. This relative agreement suggests that, given the different conditions between this study and the Fauria et al.

[2015] study, the main controls on the ability of an environment to entrap sediment are likely determined by the characteristic flow condition and size of the particles and collectors.

4.3 Influence of flocculation

This study did not consider the influence of particle flocculation on sediment removal because of the nature of the instruments. The peristaltic pump sampling method recorded the bulk sediment masses, and thus did not explicitly account for the development of flocs. Flocculation, if it occurred, was implicitly present in the mechanics of sediment removal and the observations but not directly factored into the methods and analysis.

Flocculation is expected to have a substantial role in sediment deposition because of its ability to impact settling velocities. Small particles with otherwise negligible settling velocities (“wash load”) may aggregate by flocculation into larger particles with appreciable settling velocities. These initially inconsequential particles would then need to be considered in sediment transport models over time as flocculation generates particles capable of settling within the timescale of observation. The dynamics of flocculation in suspended sediment transport require further examination in future studies, with possible extended implications for floodplain morphodynamics.

Flocculation has been found to strongly depend on the presence of saline water to inhibit interparticle repulsion, leading to the assumption that flocculation is negligible in freshwater systems [Sutherland et al., 2014]. It has also been shown that polymeric organic material and microbial activity bind particles together into flocs [Beckett and Le, 1990; Droppo et al., 1997]. Previous runs in the flume had used saline water, so residual salinity could have induced flocculation in the otherwise freshwater system in which flocculation was not expected to occur. The role of organics could not be ruled out as a potential source of flocculation because of the organic nature of the crushed walnut shell used as sediment. Previous flume runs had used sediment obtained from soils with a considerable organic fraction so residual organic components, even after cleaning, could have been involved in flocculation. As a final note, it was unclear if the presence of silicone grease interacted with the crushed walnut shell sediment to encourage flocculation. If so, silicone grease represented another potential flocculation agent in the experiments.

4.4 Study Limitations and Future Work

4.4.1 Variability and Sample Size

In the study presented here, the results were limited to two experiments. This sample size constraint was present because of the relatively intensive labor and time costs in the experimental protocol especially in installing the dowels in the flume and in filtering water samples.

Compounding the issue was the problem of variability. Additional experiments without dowels were performed at identical conditions to the no dowel treatment described in this study. However, the results of the concentration time series appeared to be different by visual inspection. Statistical comparisons of the experiments, using paired *t*-tests of paired observations at the same time and location in the flume, confirmed that they were significantly different from each other, indicating the presence of unaccounted sources of variability between ostensibly identical runs. The question of variability returns to the relatively complex protocol in which there were substantial points at which additional variability could have entered in the experiment such as potential “observer” effects of having multiple people weighing and filtering samples.

An ideal but more costly design would examine more factors (flow velocity, dowel density, presence or absence of silicone grease) at finer levels in a completely randomized

manner. At the same time, nuisance factors (e.g. run order, whether the flume was cleaned prior to a run, the number of people processing the data) should be controlled to avoid confounding with actual factors of interest. This design would also have a sufficient number of replicates within each treatment combination. An ANOVA structure would then be able to estimate effects and interactions and provide a more rigorous characterization of variance in addition to the standard calculations of capture rates and effective capture efficiency performed here. However, the high cost of the current protocol prohibited the running of the many experiments that would be required in this hypothetical design.

4.4.2 Instrument Limitations

The peristaltic pump method was used to record the sediment concentration over time in the flume at three different heights from the bed and two longitudinal locations along the flume. However, it was likely that the peristaltic pump method, and subsequent filtering protocol, lacked the sufficient precision to distinguish finer variations in sediment concentration as indicated by the absence of a significant difference in concentration between upstream and downstream sampling sites. In addition, the variability of experiment replicates as noted in the previous section may be linked to variability in the peristaltic pump method.

Future work should use a method to measure sediment concentration at greater precision and with less variability. An improved method would potentially distinguish upstream and downstream differences in sediment concentration and allow for Rouse profile analysis if information on particle size distribution would be recorded as well. Perhaps the largest benefit would be to simplify the experimental protocol to reduce unintended variability and provide a systematic quantification of instrument error variance. As a note, preliminary flume runs had used a laser scattering instrument to measure sediment volumetric concentration over time with the ability to distinguish particle size distributions, but uncertainties about instrument integrity had precluded its further use.

In this study, a statistical estimation method was used to infer the size distribution of the crushed walnut shell because of instrument constraints. One improvement would be to directly measure the size distribution using a particle analyzer, so that a size distribution representative of the actual sample of sediment available could be obtained.

4.4.3 Error Analysis

A shortcoming of the methods in this study was the inability to adequately assess error at the experiment level. This was directly a result of the lack of replicates for the experiments. Additional data from replicates would permit the assessment of variability at the scale of an experiment. In this study, particle capture rate and its associated parameters (capture rate due to settling, capture rate due to direct interception, effective capture efficiency) were assigned uncertainty bounds due to the model fit. However, these quantities refer to variability within the conditions of the specific experiment and not at the general scope of runs with identical flume settings.

Despite the availability of error quantification for some parameters, errors remained underdetermined for others. The model standard error for k was propagated through each calculation of k_s , k_c , and η' . However, other variables in the computations were subject to error as well but not accounted for in the error (e.g. m_s from sediment trap data). The uncertainty in these parameters was insufficiently characterized and, as a result, underestimated.

Another issue is the need for rigorous error control throughout the protocol to ensure that systematic bias between runs is as small as possible, for example the potential “observer” effects

mentioned earlier. The minimization of these procedural errors is needed to avoid the presence of possible lurking, unaccounted factors that inflate variability in results. Replicates of the no dowel treatment described in this study have been observed to be significantly different from each other, indicating an unknown additional source of variability that may relate to slight inconsistencies in protocol between runs.

5 Conclusion

References

- Beckett, Ronald, and Ngoc P. Le. 1990. "The Role of Organic Matter and Ionic Composition in Determining the Surface Charge of Suspended Particles in Natural Waters." *Colloids and Surfaces* 44 (January): 35–49. [https://doi.org/10.1016/0166-6622\(90\)80185-7](https://doi.org/10.1016/0166-6622(90)80185-7).
- Britsch, Louis D., and Joseph B. Dunbar. 1993. "Land Loss Rates: Louisiana Coastal Plain." *Journal of Coastal Research* 9 (2): 324–38.
- Brownlie, William R. 1981. "Prediction of Flow Depth and Sediment Discharge in Open Channels." Report or Paper. November 1981. <http://resolver.caltech.edu/CaltechKHR:KH-R-43A>.
- Droppo, I. G., G. G. Leppard, D. T. Flannigan, and S. N. Liss. 1997. "The Freshwater Floc: A Functional Relationship of Water and Organic and Inorganic Floc Constituents Affecting Suspended Sediment Properties." In *The Interactions Between Sediments and Water: Proceedings of the 7th International Symposium, Baveno, Italy 22–25 September 1996*, edited by R. Douglas Evans, Joe Wisniewski, and Jan R. Wisniewski, 43–53. Dordrecht: Springer Netherlands. https://doi.org/10.1007/978-94-011-5552-6_5.
- Fauria Kristen E., Kerwin Rachel E., Nover Daniel, and Schladow S. Geoffrey. 2015. "Suspended Particle Capture by Synthetic Vegetation in a Laboratory Flume." *Water Resources Research* 51 (11): 9112–26. <https://doi.org/10.1002/2014WR016481>.
- García, Marcelo H. n.d. "Sedimentation Engineering - Processes; Measurements; Modeling; and Practice - ASCE Manuals and Reports on Engineering Practice (MOP) No. 110." <https://app.knovel.com/hotlink/toc/id:kpSEPMMP02/sedimentation-engineering/sedimentation-engineering>.
- Kadlec Robert H. 1990. "Overland Flow in Wetlands: Vegetation Resistance." *Journal of Hydraulic Engineering* 116 (5): 691–706. [https://doi.org/10.1061/\(ASCE\)0733-9429\(1990\)116:5\(691\)](https://doi.org/10.1061/(ASCE)0733-9429(1990)116:5(691)).
- Nepf, H. M. 1999. "Drag, Turbulence, and Diffusion in Flow through Emergent Vegetation." *Water Resources Research* 35 (2): 479–89. <https://doi.org/10.1029/1998WR900069>.
- Palmer Molly R., Nepf Heidi M., Pettersson Thomas J. R., and Ackerman Josef D. 2004. "Observations of Particle Capture on a Cylindrical Collector: Implications for Particle Accumulation and Removal in Aquatic Systems." *Limnology and Oceanography* 49 (1): 76–85. <https://doi.org/10.4319/lo.2004.49.1.0076>.
- Sutherland, Bruce R., Kai J. Barrett, and Murray K. Gingras. 2015. "Clay Settling in Fresh and Salt Water." *Environmental Fluid Mechanics* 15 (1): 147–60. <https://doi.org/10.1007/s10652-014-9365-0>.
- Syvitski, James P. M., Albert J. Kettner, Irina Overeem, Eric W. H. Hutton, Mark T. Hannon, G. Robert Brakenridge, John Day, et al. 2009. "Sinking Deltas Due to Human Activities." *Nature Geoscience* 2 (10): 681–86. <https://doi.org/10.1038/ngeo629>.
- Wu, Lei, Bin Gao, and Rafael Muñoz-Carpena. 2011. "Experimental Analysis of Colloid Capture by a Cylindrical Collector in Laminar Overland Flow." *Environmental Science & Technology* 45 (18): 7777–84. <https://doi.org/10.1021/es201578n>.